Understanding Ion Charging Dynamics in Nanoporous Carbons for Electrochemical Double Layer Capacitor Applications

Kangkang Ge, Hui Shao, Pierre-Louis Taberna, Patrice Simon

Understanding Ion Charging Dynamics in Nanoporous Carbons for Electrochemical Double Layer Capacitor Applications

Kangkang Ge,[1,2] Hui Shao[1,2] Pierre-Louis Taberna[1,2] and Patrice Simon[1,2]**

1.Université Paul Sabatier, CIRIMAT UMR CNRS 5085, 118 Route de Narbonne, 31062 Toulouse, France

2.Réseau sur le Stockage Electrochimique de l'Energie (RS2E), FR CNRS 3459, France

Corresponding Authors

Pierre-Louis Taberna: pierrel-louis.taberna@univ-tlse3.fr

Patrice Simon: patrice.simon@univ-tlse3.fr

ABSTRACT: The electric double layer (EDL) is one of the key concepts in electrochemistry and understanding its charging kinetics is of key importance. Significant progress has been made via theoretical methods; however, it is challenging to study the ion dynamics experimentally in porous carbon electrodes under realistic conditions because of fast charge relaxation. In this work, the charging kinetics of porous carbon electrodes with different pore sizes in the aqueous

electrolyte was experimentally investigated in electrolytes with various concentrations by using a cavity micro-electrode. We were able to observe electrolyte depletion and we systematically studied the key parameters that will affect the electrolyte depletion, resulting in major changes in the charging kinetics. Results showed that low concentration, high overpotential potential and small carbon pore size triggered the electrolyte depletion, decreasing the charging kinetics. These findings further push our understanding of the ion dynamics of EDL at charged porous carbon/electrolyte interface.

TOC GRAPHICS

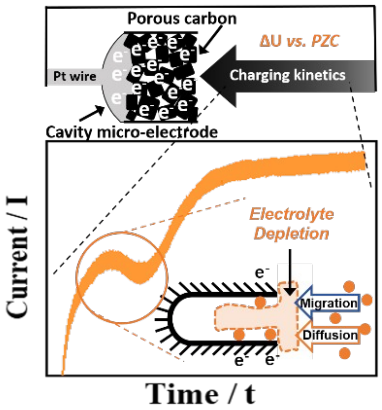

Understanding the formation of the electric double layer (EDL) at porous carbon electrode/electrolyte interface is of high importance in various applications such as energy storage (electrochemical double-layer supercapacitors),[1] capacitive deionization,[2-4] or energy harvesting.[5-7] Classical planar EDL theory, so-called the Gouy-Chapman-Stern model, has been

established using two parallel charged planar electrodes immersed in an electrolytic solution,[8] with the Poisson-Nernst-Plank (PNP) equation to address time-dependent charge-relaxation phenomena.[9] Nevertheless, moving from 2D planar to a high surface area porous electrode comes with confinement effect,[10-11] presence of chemical defects[12], potential distribution, curvature effects[13] (…) that make porous electrode behavior different from classical planar ones. A few decades ago, de Levie first proposed a transmission line model (TLM), which considers uniformly distributed capacitance and solution resistance throughout the pores, to model the charge storage behaviors in porous carbon.[14] TLM and their associated equivalent circuits are widely used to describe the frequency behavior under small potential bias in porous carbon electrodes by catching the linear or the early-times nonlinear kinetics.[9, 15] To move further, new theoretical models have been proposed. Indeed, the required voltage for a realistic EDL charging process up to about 1.0V in aqueous electrolyte[16] is always larger when compared to 25 mV (RT/F~25 mV at room temperature), which is the potential derived from the linear approximation of PNP equation[15, 17], above which potential the mathematic calculations are challenged. Therefore, Biesheuvel and Bazant[18] derived nonlinear porous-electrode equations and found two domains. At small voltages or early times, a porous electrode acts like a transmission line, governed by a linear diffusion equation that results in a potential distribution inside the porous carbon network; while for large voltages and long times, porous electrode kinetics is governed by coupled, nonlinear diffusion equations and local electrolyte depletion[18]. Conway[19] depicted an electrolyte concentration depletion when there is a limited amount of electrolyte ions at the charged porous carbon/electrolyte interface and pointed out its negative effect on the local ionic conductivity—resulting in power performance limitation. Besides, the increased electrolyte resistance caused by electrolyte depletion makes the charging kinetics

slower and nonlinear.[17-18] Later, Lian and co-workers[20] proposed a parallel stacked electrode model to describe the carbon charging kinetics. They confirmed the existence of the two relaxation time domains, with the RC relaxation (TLM) at early times or low voltages, and a diffusion limitation domain at longer times. This model well bridged a 5-order of magnitude gap between single slit pore simulation and experimentally observed relaxation time constant at the electrode level. But the key parameters such as finite ion size and pore length/morphology should also be taken into account. Since recently, models have been refined to get closer to actual three-dimensional confinement systems, such as chemically driven charge localization (CDCL) model[12], modified PNP model,[21-22] and dynamic density functional theory (DDFT)[23]… Together with experimental parameters (for instance the finite pore length,[22, 24] pore size distribution,[25] curvature,[13] ion confinement,[10, 26] desolvation and defects[12]), it greatly contributes to the theoretical understanding of ion transport kinetics in porous carbon electrodes. However, experimental approaches are barely proposed to further validate these theoretical approaches, and experimental investigations of the EDL formation and evolution for the subnanopores with confinement are highly desired.

The major obstacle that hinders experimental tracking of ionic dynamics is the fast charge relaxation, namely the fast charge separation and charging of EDL resulting from the electrostatic nature of the charge storage. Dilute electrolyte solutions with lower ionic conductivity are preferred to slow down ion dynamics in order to track the small charging kinetic differences. Also, the use of micro-electrode should be preferred in low electrolyte concentrations to limit the ohmic drops and allow for the electrochemical kinetics study. For instance, Zuleta[27-29] and co-workers determined the effective diffusion coefficient in porous carbon using a single particle micro-electrode technique. Besides, cavity micro-electrode (CME)

was found interesting in exploring electrochemical kinetics of various materials for energy storage applications such as lithium iron phosphate (LFP),[30-31] MXenes 2D metal carbides[32] and porous.[33]

In this work, carbide-derived carbons (CDCs) with high surface area, tunable porosity, controllable average pore size and narrow pore size distributions were used as model porous carbon materials for revealing the EDL charging mechanisms under confinement.[34] The use of a CME made it possible to reveal the fundamental electrochemical kinetic behaviors.[35] While previous works proposed theoretical approaches built on models describing salt depletion and charge relaxation time scales at largely applied potentials, we provide for the first time, to the best of our knowledge, direct observation of the electrolyte depletion process and a systematic study to show how the electrolyte depletion affects the charging kinetics. The set of results provided here shed light on ion transport and adsorption kinetics at a realistic, charged porous carbon / electrolyte interface.

The Cavity Micro-Electrode (CME) used here consists of a Pt wire embedded inside a silica glass tube. After polishing and controlled dissolution of the Pt wire, a small cavity of ~50 μm diameter and ~20μm depth is prepared, where about 10^{-7}-10^{-8} g of active material powder can be packed[36] (Figure S1), without the need for conductive additives or binders. **Figure 1** shows the cyclic voltammetry (CV) curves of CDC porous carbons in a three-electrode configuration using the CME as a working electrode. The current in CVs was normalized to the potential scan rate[37]. In conventional 1.0 M of Li_2SO_4 electrolyte, all normalized CVs exhibit a symmetric and rectangular shape at all scan rates (0.2, 0.5 and 1.0 V s^{-1} see **Figure 1a**), indicating a reversible

ion adsorption/desorption process with fast ion transport kinetics, as expected for porous carbon electrodes. It also confirms the negligible ohmic drop observed using the CME. The fast kinetics stems from the fast ion transport and ion adsorption and desorption processes.

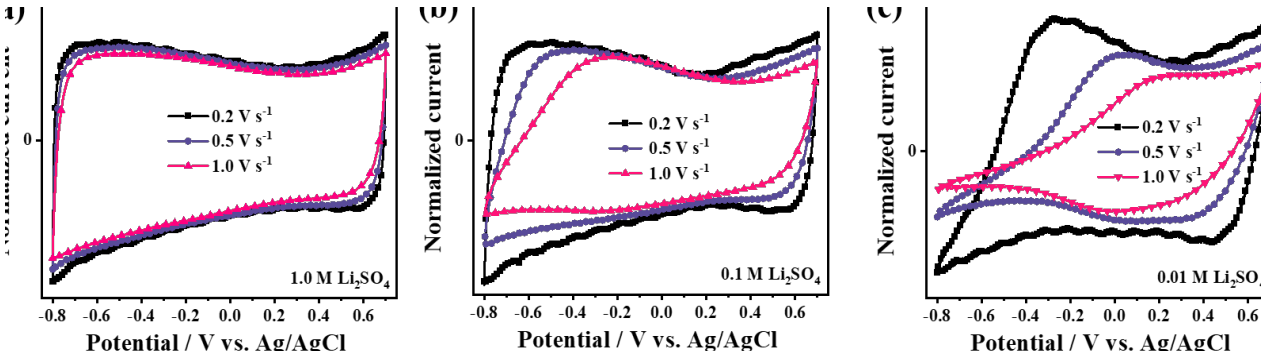

Figure 1. Cyclic voltammetry plots of CDC-600 °C in Li_2SO_4 electrolyte were obtained using a cavity micro-electrode at scan rates of 0.2 V s^{-1}, 0.5 V s^{-1} and 1.0 V s^{-1}. The electrolyte concentrations are (a) 1.0 M Li_2SO_4, (b) 0.1 M Li_2SO_4 and (c) 0.01 M Li_2SO_4.

When the electrolyte concentration is decreased by ten times from 1.0 M to 0.1 M, the rectangular shape still remains at a lower scan rate, that is 0.2 V s^{-1} in our case, while obvious distortion appears at elevated scan rates (**Figure 1b**). The asymmetry of the CV distortion (Figures 1b and 1c) as well as the low current value passed in the electrode (for example, 600 nA at 0.2 V s^{-1}) supports the kinetic origin of these limitations.[37] Indeed, an important limitation (drastically reduced current) is observed in 0.01 M Li_2SO_4 electrolyte during negative polarization (below -0.2 V vs. Ag/AgCl, 0.5 V s^{-1}). This limitation is not fully ohmic in nature as the positive polarization is much less affected (**Figure 1c**)—the distortion is not symmetric as expected for an ohmic limitation—as the result of the different ion species involved in the charge

storage mechanism during positive and negative polarization[37-38]. The current decrease could arise from local electrolyte depletion, which can only be observed in a specific range of concentration, since for high-concentration electrolytes, adsorbed ion amount is barely noticeable and the depletion space is expected to be fed quickly whereas too low concentration would lead to a resistive signal.[17] Therefore, the unique electrochemical signature of CDC in Li_2SO_4 electrolyte obtained at low concentration could be used to emphasize the electrolyte depletion and the ion dynamics during charge/discharge of the EDL in microporous carbons.

To further investigate the electrolyte depletion and its impact on charging kinetics, the current change over time was monitored during potential step experiments (chronoamperometry, set up is shown in Figure S2). More specifically, the potential of the porous CDC electrode was set at the potential of zero charge (PZC), we measured it at the minimum current from the cyclic voltammograms; then, a negative constant potential was applied with respect to the PZC and the current change vs. time was recorded. The PZC of CDC-600 °C was measured at about 0.2 V vs. Ag/AgCl in 0.01 M Li_2SO_4 electrolyte (see Figure S3). In fact, the PZC of CDCs should be very close to the open circuit potential before any electrochemical test, as CDCs are free of functional groups[37, 39]. As expected, it is the same whatever the electrolyte concentration in our study—although it is more accurately detected for the lowest concentration, as the minimum capacitance is more pronounced. As the pH of the electrolyte was measured at around 6, all the charges accumulated during the negative potential polarization step should then be mainly associated with Li^+ adsorption with negligible SO_4^{2-} ion exchange[40].

Figure 2a shows the current response with time, once the electrode was polarized from PZC to -1.2 V vs. PZC. In highly concentrated electrolyte (1.0 M Li_2SO_4), the cathodic current decay follows the expected exponential decrease characteristics of a capacitive (electrostatic) charge storage by ion adsorption. Different behaviors were then observed in 0.1 M, 0.01 M and 0.005 M electrolytes, with non-monotonous current decays, are observed and the presence of current peaks in some cases. Those observations may be consistent with a more complex charge mechanism likely linked with electrolyte depletion. Indeed, just after polarization the current varies as expected for a capacitive electrode, exponentially, then it increases and decreases—current peak—until the carbon is fully charged. Interestingly, the position of the current peak depends on the electrolyte concentration—it shows up later when the electrolyte concentration is lower.

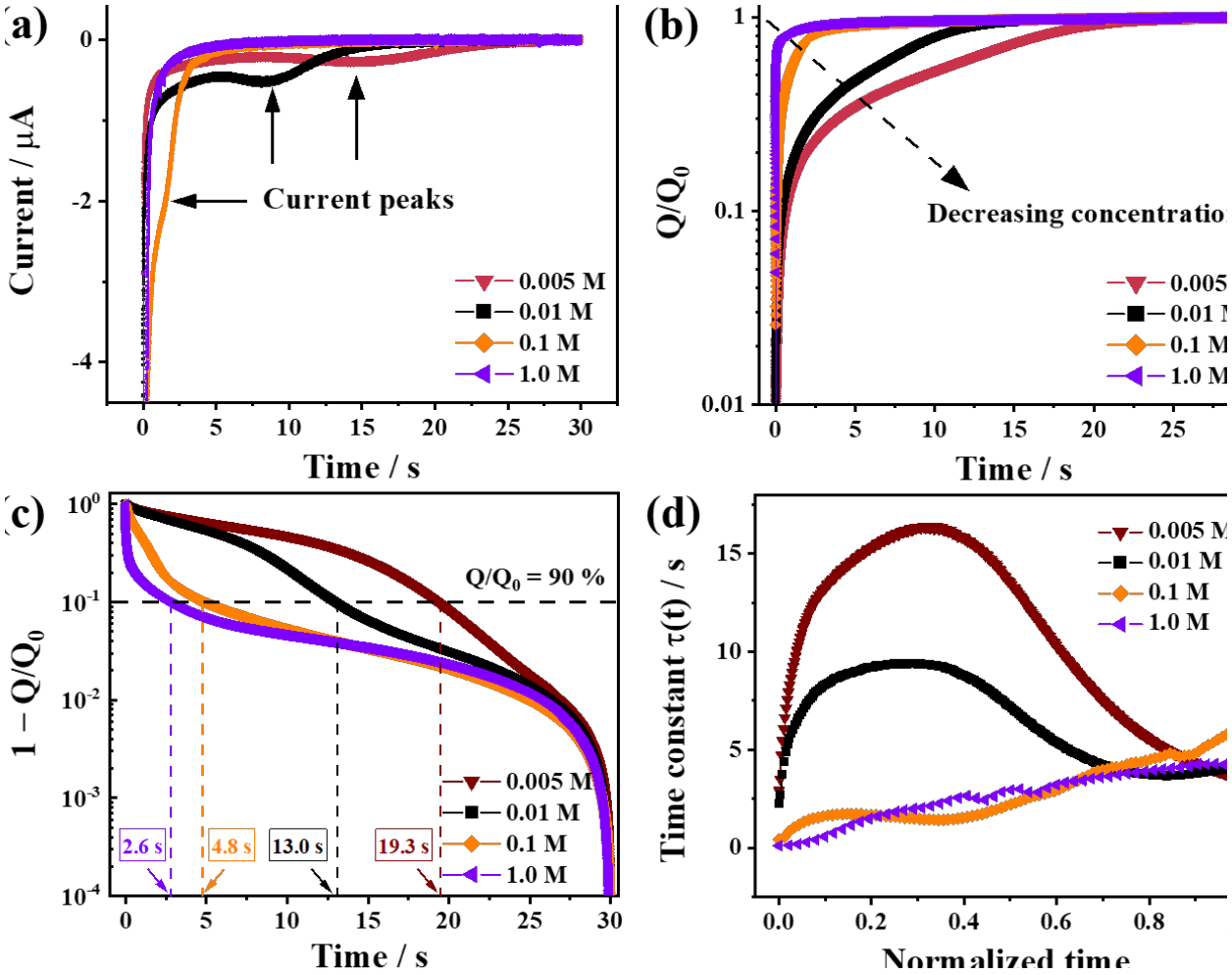

Figure 2. Change of the charging kinetics of CDC-600 at a holding potential of -1.2 V vs. PZC in Li_2SO_4 electrolyte, with concentrations ranging from 0.005 M to 1.0 M. (a) Current response and (b) cumulative normalized charge (Q/Q_0) change with time obtained by integration of the plots in (a). (c) Semilog plot of $1-Q/Q_0$ change with time. (d) Transient charging time constants ($[-dLn(1-Q/Q_0)/dt]^{-1}$) change with normalized time (time normalized to time corresponds to 90% of Q/Q_0) along the whole charging process.

For electrolytes with a high ionic concentration, the current is driven by the migration of ions —no concentration limitation—and changes exponentially; for electrolytes having a low ionic

concentration, the current is first driven by the migration flow until ionic depletion occurs leading to a high concentration gradient. As a result, a diffusion current adds up, which may explain a current peak shows up. Interestingly, the phenomenon is more severe for 0.005M than for 0.01M, resulting in a current peak at a longer time when decreasing the electrolyte concentration (Figure 2a). Once the permanent regime is established, the current continuously decays to reach a steady state, at which state the surface charge is mostly screened by electrolyte ions. Figure S4 shows the cumulative charge obtained by integrating the current with the time plots of Figure 1a. Owing to the small leakage current existing in realistic porous carbon electrodes (being not ideally polarizable, as the result of the possible presence of small amounts of redox active impurities on the carbon surface and charge distribution), the background in Figure S4 has been subtracted by removing the average stabilized leakage current of the last two seconds to ensure that the calculated charge corresponds only to the reversible capacitive process. In Figure S4, it is worth noting the maximum charge is directly correlated with the ionic concentration, which is in line with an ionic concentration limitation.

For better comparison of the kinetics, the cumulative capacitive charges were normalized to the total charge at 100 % charge state (defined as Q_0), which is the charge calculated at the end of the test, as confirmed by the roughly constant value of the cumulative charge in Figure S5. As expected, the cumulative charge varies with the electrolyte concentration (Figure S5); more specifically, lower concentration delays the charge storage as shown in Figure 2b (Q/Q_0 vs. time), which means the full charge state of the carbon electrode is reached at longer times in low

concentration electrolytes. **Figure 2b** clearly shows a huge charging rate difference at an early time, where the electrolyte depletion occurs, as shown in the ($1-Q/Q_0$) vs. time plot (**Figure 2c**). The change of the cumulative charge Q was plotted as $1-Q/Q_0$, to better define the early time charging kinetics. In the rest of this work, we will consider that 90 % state of charge (SOC) of the carbon electrodes is representative of a fully charged system, as the extra 10 % charge would need a long time due to the exponential decay of the current. It takes only 2.6 s to reach 90 % of Q/Q_0 for 1 M electrolyte while 4.8 s, 13.0 s and 19.3 s are needed to reach the same state of charge, respectively in 0.1 M, 0.01 M and 0.005 M electrolyte. To further study the charging kinetics, we derivated the $Ln(1-Q/Q_0)$ vs. time plot and defined a transient charging time constant τ_t as (equation (1), and equation S1-S5):

$$\tau_t = \left[- \frac{dLn(1 - Q/Q_0)}{dt} \right]^{-1} \quad \text{equation (1)}$$

The change of τ_t with the charging time t was plotted to better understand the transient kinetics —a dimensionless time was used, corresponding to the actual time divided by the time to reach a state of charge of 90 % (equation 2).

$$\text{Normalized time } t_N = \frac{t}{t_{Q/Q_0=90\%}} \quad \text{equation (2)}$$

Figure 2d gives the change of time constant for the different electrolyte concentrations, where different behaviors can be observed. For the highly concentrated 1.0 M electrolyte, a monotonic increase of the time constant was found, showing increases from 0 to less than 4 s. This change is in line with a time constant distribution as expected for a porous electrode. Interestingly, for the

electrolytes with lower concentration, a time constant peak/bump is observed for short times—in the case of 0.1 M, it is followed by a monotonic increase. This peak is assumed to be related to the electrolyte depletion, as a result of the limited amount of ionic species close to the carbon surface. Although it is barely visible for the electrode tested in 0.1 M electrolyte, as on average it behaves roughly as the electrode in 1 M electrolyte, it is very obvious for the lowest electrolyte concentrations. It is worth noting for those concentrations, the time constant peak is then followed by a time constant in the order of magnitude than the other concentrations. For 1 M and 0.1 M electrolytes, the charging process is mainly driven by the ion migration and successive time constants are supposed to be observed as it is a porous electrode. Concerning the 0.01 M and 0.005 M electrolytes, an ionic depletion is present, leading to an ion diffusion flux toward the electrode that adds up to the ion migration flux—this is assumed to translate into the current peak observed in Figure 2a. Such process only appears in low-concentration electrolytes (<0.1 M), since there is no depletion effect in 1 M electrolyte. Beyond being in agreement with previous modeling works, those results allow for the experimental observation of the plateau region for τ_t which is related to the time constant of the diffusion process of the ions to reach the adsorption sites on the electrode surface[15, 22]. The observed shift to a longer time of the plateau when decreasing the electrolyte concentration is the result of increased diffusion limitation[20]. Therefore, the plateau is only slightly visible when electrolyte concentration is lowered down to 0.1 M, but is the main feature when further decreasing the electrolyte concentration down to 0.01 M and 0.005 M. As mentioned above, the 0.1 M electrolyte concentration shows an intermediate

behavior, with a delay in the charge storage process vs. the highly concentrated 1 M electrolyte (4.8 s vs. 2.6 s to reach 90 % SOC, Figure 2c) but without a clear plateau for τ_t, showing that 0.1 M ion concentration is still high enough to drastically decrease the diffusion limitation under our experimental conditions.

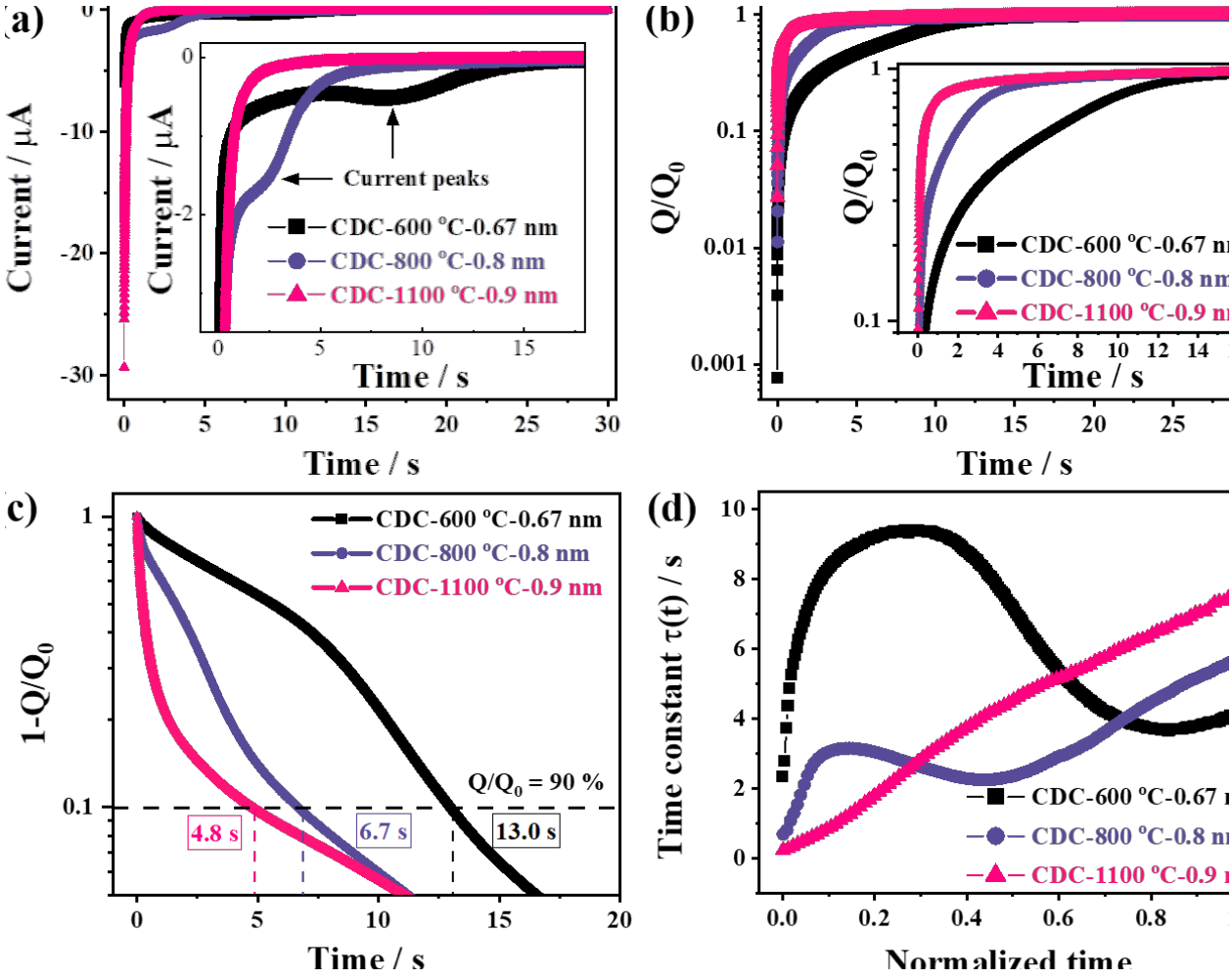

Figure 3. Pore size dependent charging kinetics of CDC with potential holding at -1.2 V vs. PZC in 0.01 M Li_2SO_4 electrolyte. (a) Current response and (b) cumulative normalized charge (Q/Q_0) change with time obtained by integration of the plots in (a). (c) Semilog plot of $1-Q/Q_0$ change

with time. (d) Transient charging time constants ($[-d\ln(1-Q/Q_0)/dt]^{-1}$) change with normalized time (time normalized to time corresponds to 90% of Q/Q_0) along the whole charging process.

In the next step, the influence of the applied potential on the depletion and charging kinetics was studied by polarizing the carbon electrode at different constant cathodic potentials vs. PZC, in 0.01 M Li_2SO_4 electrolyte. Figure S6 shows the change of the current during the constant potential step. The profile is similar to Figure 1a, and an exponential decay of the current is observed during the first second of the polarization as a result of the fast charge process, followed by a current increase when increasing the cathodic overpotential. Such current increase demonstrates that higher cathodic overpotentials result in severe electrolyte depletion: the ion populations near or inside the carbon pores can no longer meet the required amount of ions to screen the applied potential. Consequently, a current peak is observed for a potential of -1.2 V vs. PZC, in the same way as what was observed with decreasing electrolyte concentrations. Therefore, we fixed the overpotential at -1.2 V vs. PZC to study the pore size effect on the depletion and related charging kinetics.

Porous carbon materials (CDCs) were prepared by chlorination of TiC powders [41,42], where the chlorination temperature controls the carbon pore size. CDC-600°C, CDC-800 °C and CDC-1100 °C with average pore sizes of 0.67 nm, 0.8 nm and 0.9 nm (Table S1), respectively, were prepared and used as model materials to investigate the effect of the pore size on the charging kinetics. The SEM images showed similar morphology of the porous carbon grains, with grain sizes around 5-10 μm for all the samples (Figure S7). **Figure 3a** shows the current response with

time during the polarization from PZC to -1.2 V vs. PZC of the CDC with different pore sizes. The current peaks related to electrolyte depletion are observed at 2.5 s and 8.5 s for CDC-800°C (0.8 nm) and CDC-600°C (0.67 nm), respectively, as a result of the small pore size. The peak disappears for the large pore size of 0.9 nm (CDC-1100 °C).[43] As expected, a slower charge accumulation rate was observed with decreasing the carbon pore size (**Figure 3b**), in agreement with former experimental observation in non-aqueous electrolytes[37-38]. Previous computational works[34, 44] also predicted that smaller average pore size results in a slower charging rate at the molecular level. The characteristic charging times to reach 90% SOC were found to range from 0.5 to 4 s, which is also in good agreement with those predicted.[34] The pore size-dependent charging kinetics could be attributed to steric hindrance of the pore accessibility[37-38, 42, 45-47] and/or to the ion desolvation process.[12] The solvation shell of Li^+ in aqueous electrolytes usually contains 5 to 6 H_2O molecules with a Li-O distance (3.5-4.0 Å) for the second hydration shell[48-49], making solvated Li^+ ion sensitive to steric hindrance during transport in subnanometer pores of the porous carbon network. Therefore, the sluggish adsorption kinetics observed for narrow pores could be explained by the hindered transportation of solvated Li^+, together with their partial desolvation process when accumulated in the subnanometer carbon pores[39, 50].

Similarly, to further investigate the depletion-related charging kinetics, we plotted $1 - Q/Q_0$ vs. time with different pore-sized CDCs. It takes 4.8 s to reach 90 % of Q/Q_0 for cabrons with bigger pore size, while the time is delayed to 6.7 s and 13.0 s for smaller pore size one (**Figure 3c**). The change of τ_t vs. normalized time shown in **Figure 3d** was used to better highlight the difference

in charging kinetics. Similar change of τ_t as reported in Figure 2d were observed as well, in relation to electrolyte depletion, but only for carbons with a pore size below 0.9 nm. In Figure 3d, the transient time constant τ_t slowly increases for the 0.9 nm sample, which is consistent with the absence of any electrolyte depletion and is controlled by the potential distribution inside the carbon pores due to the RC relaxation (TLM model). Similarly to what was observed in Figure 2d, a time constant bump appears for smaller pore sizes, with a higher average τ_t value with decreasing pore size. The electrolyte depletion is only present for small pore size samples and is likely to occur as subnanopores are more easily depleted than larger pores—the pore size being smaller, the total available ions nearby the carbon surface being lower. Also, the ion transport is expected to be slower.

Based on the results discussed above, we could propose a view (**Figure 4**) of the charging process in porous carbon when electrolyte depletion occurs. At the open circuit potential (OCP), there is no ion concentration gradient in the bulk electrolyte (**Figure 4a**). When applied an electrical potential difference, the external surface or the orifice of the pores will be first charged before the inner porous network.[14] In the case of electrolyte depletion occurs, that could be triggered by higher applied potential, lower electrolyte concentration or smaller average pore size-the limitation of ion transportation, it results in electrolyte depletion inside the subnanopores and on the external surface, as discussed previously.[17] Then, a mass transfer film adjacent to the electrode was formed and extended into the pore, which is also called the "stagnant diffusion layer (SDL)" elsewhere.[18] In this case, the ion diffusion and ion migration contribute together to

the charge accumulation (**Figure 4b**). Meanwhile, the limited ion transportation within the depleted area pushes the charge storage process delayed to longer times. At longer times, it reaches the steady charging state of EDL, where the ions migrate toward charged carbon surface and ion diffusion started from carbon surface and extends to the bulk electrolyte and they reach a dynamic balance at the end of charging steady state (**Figure 4c**). However, there is no electrolyte depletion in a conventional view, that is, in the case of high electrolyte concentrations, small potential bias and/or large pore size. After polarization, the ion concentration and potential gradients then develop inside the pores and in the bulk solution near the external surface as a result of the ion adsorption process.[18]

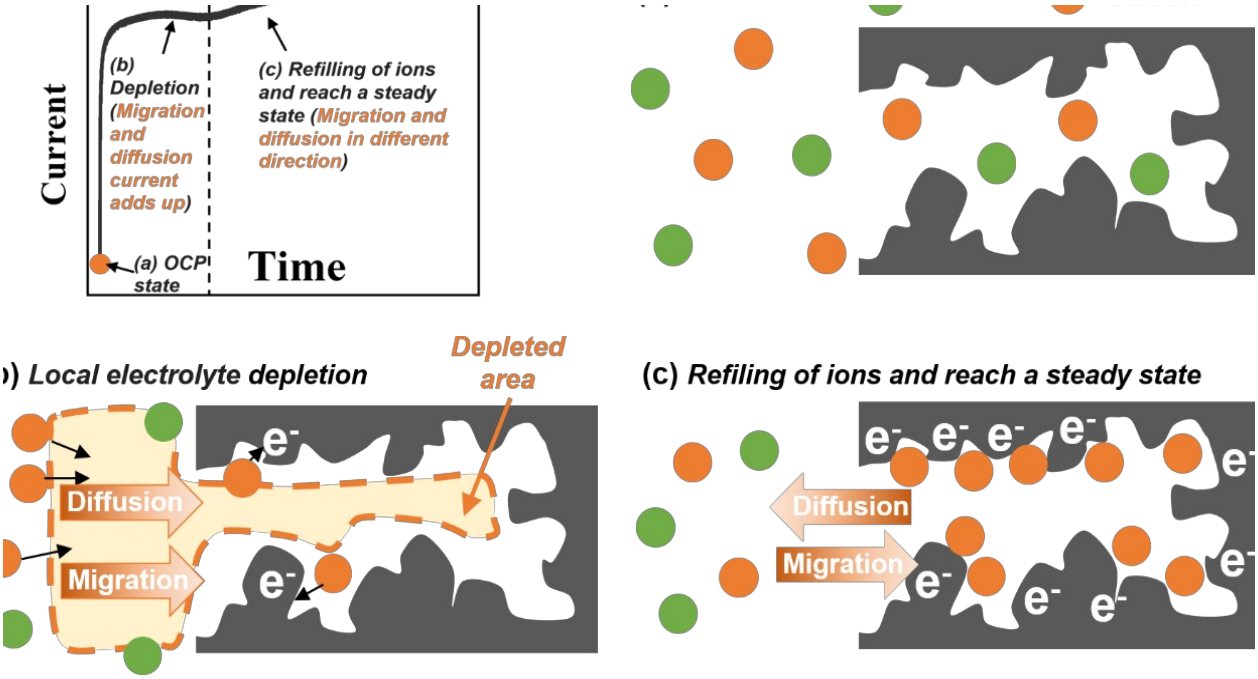

Figure 4. Schematic illustration of the charging process of porous carbon when electrolyte depletion occurs. (a) At PZC state, there are no extra ions absorbed by electrostatic interaction on

the carbon surface. (b) The early time charge accumulation occurs when electrolyte depletion occurs near the polarized electrode surface. Sluggish kinetics emerges in the depleted area, and meanwhile the migration and diffusion current adds up. (c) Charge accumulation at a charged porous carbon/electrolyte interface in a steady state where ion migration and diffusion head in the opposite direction.

In conclusion, the EDL charging kinetics of microporous carbons with various porosity was experimentally investigated in aqueous electrolytes with different ion concentrations. The use of a cavity micro-electrode helped minimizing the ohmic drops and allowed us to experimentally observe and characterize the electrolyte depletion inside the porous carbon network, responsible for sluggish EDL charging kinetics. We also pointed out several parameters that affect this depletion, such as the pore size, electrolyte concentration and the applied cathodic overpotential. The set of results allows for a better understanding of the ion dynamics and EDL charging in porous carbon electrodes from an experimental approach, which confirms some recent models predicted by theoretical approaches. Our findings can also help to design experimental set-ups and simulation conditions for further studying the EDL charging behavior in realistic electrodes.

Supporting Information. Electrochemical techniques, equations, set up, additional electrochemical data and carbon material characterization.

AUTHOR INFORMATION

Corresponding Authors

Pierre-Louis Taberna− Université Paul Sabatier, CIRIMAT UMR CNRS 5085, 118 Route de Narbonne, 31062 Toulouse, France; Email: pierrel-louis.taberna@univ-tlse3.fr

Patrice Simon− Université Paul Sabatier, CIRIMAT UMR CNRS 5085, 118 Route de Narbonne, 31062 Toulouse, France; Email: patrice.simon@univ-tlse3.fr

Authors

Kangkang Ge − Université Paul Sabatier, CIRIMAT UMR CNRS 5085, 118 Route de Narbonne, 31062 Toulouse, France; Email: kangkang.ge@univ-tlse3.fr

Hui Shao − Université Paul Sabatier, CIRIMAT UMR CNRS 5085, 118 Route de Narbonne, 31062 Toulouse, France; Email: hui.shao@univ-tlse3.fr

Notes

The authors declare no competing financial interest.

ACKNOWLEDGMENT

K.G. was supported by a grant from the China Scholarship Council (no. 202006340020). H.S., P.S. and P.L.T. acknowledge the support from Agence Nationale de la Recherche (Labex Store-ex) and ERC Synergy Grant MoMa-Stor #951513.

REFERENCES

(1) Simon, P.; Gogotsi, Y., Perspectives for electrochemical capacitors and related devices. *Nature Materials* **2020,** *19* (11), 1151-1163.

(2) Rubin, S.; Suss, M. E.; Biesheuvel, P. M.; Bercovici, M., Induced-Charge Capacitive Deionization: The Electrokinetic Response of a Porous Particle to an External Electric Field. *Phys. Rev. Lett.* **2016,** *117* (23), 234502.

(3) Rica, R. A.; Ziano, R.; Salerno, D.; Mantegazza, F.; Brogioli, D., Thermodynamic relation between voltage-concentration dependence and salt adsorption in electrochemical cells. *Phys. Rev. Lett.* **2012,** *109* (15), 156103.

(4) Zhang, Y.; Prehal, C.; Jiang, H. L.; Liu, Y.; Feng, G.; Presser, V., Ionophobicity of carbon sub-nanometer pores enables efficient desalination at high salinity. *Cell Rep Phys Sci* **2022,** *3* (1), 100689.

(5) Brogioli, D., Extracting Renewable Energy from a Salinity Difference Using a Capacitor. *Phys. Rev. Lett.* **2009,** *103* (5), 058501.

(6) Emmerich, T.; Vasu, K. S.; Nigues, A.; Keerthi, A.; Radha, B.; Siria, A.; Bocquet, L., Enhanced nanofluidic transport in activated carbon nanoconduits. *Nature Materials* **2022,** *21* (6), 696-702.

(7) Simoncelli, M.; Ganfoud, N.; Sene, A.; Haefele, M.; Daffos, B.; Taberna, P. L.; Salanne, M.; Simon, P.; Rotenberg, B., Blue Energy and Desalination with Nanoporous Carbon Electrodes: Capacitance from Molecular Simulations to Continuous Models. *Phys Rev X* **2018,** *8* (2), 021024.

(8) Shao, H.; Wu, Y. C.; Lin, Z. F.; Taberna, P. L.; Simon, P., Nanoporous carbon for electrochemical capacitive energy storage. *Chem Soc Rev* **2020,** *49* (10), 3005-3039.

(9) Sakaguchi, H.; Baba, R., Charging dynamics of the electric double layer in porous media. *Phys. Rev. E Stat. Nonlin. Soft Matter Phys.* **2007,** *76* (1 Pt 1), 011501.

(10) Pean, C.; Daffos, B.; Rotenberg, B.; Levitz, P.; Haefele, M.; Taberna, P. L.; Simon, P.; Salanne, M., Confinement, Desolvation, And Electrosorption Effects on the Diffusion of Ions in Nanoporous Carbon Electrodes. *J. Am. Chem. Soc.* **2015,** *137* (39), 12627-12632.

(11) Merlet, C.; Pean, C.; Rotenberg, B.; Madden, P. A.; Daffos, B.; Taberna, P. L.; Simon, P.; Salanne, M., Highly confined ions store charge more efficiently in supercapacitors. *Nat. Commun.* **2013,** *4*, 1-6.

(12) Dupuis, R.; Valdenaire, P. L.; Pellenq, R. J.; Ioannidou, K., How chemical defects influence the charging of nanoporous carbon supercapacitors. *Proc. Natl. Acad. Sci. U.S.A.* **2022,** *119* (17), e2121945119.

(13) Seebeck, J.; Merlet, C.; Meissner, R. H., Elucidating Curvature-Capacitance Relationships in Carbon-Based Supercapacitors. *Phys. Rev. Lett.* **2022,** *128* (8), 086001.

(14) Levie, R. d., On Porous Electrodes in Electrolyte Solutions. *Elecrrochim. Acta* **1963,** *8*, 751-780.

(15) Bazant, M. Z.; Thornton, K.; Ajdari, A., Diffuse-charge dynamics in electrochemical systems. *Phys. Rev. E Stat. Nonlin. Soft Matter Phys.* **2004,** *70* (2 Pt 1), 021506.

(16) Aslyamov, T.; Sinkov, K.; Akhatov, I., Relation between Charging Times and Storage Properties of Nanoporous Supercapacitors. *Nanomaterials (Basel)* **2022,** *12* (4), 587.

(17) David B. Robinson; Chung-An Max Wu; Jacobs, B. W., Effect of Salt Depletion on Charging Dynamics in Nanoporous Electrodes. *J. Electrochem. Soc.* **2010,** *157*, A912-A918.

(18) Biesheuvel, P. M.; Bazant, M. Z., Nonlinear dynamics of capacitive charging and desalination by porous electrodes. *Phys. Rev. E Stat. Nonlin. Soft Matter Phys.* **2010,** *81* (3 Pt 1), 031502.

(19) Conway, B. E., *Electrochemical supercapacitors: scientific fundamentals and technological applications*. Springer New York, NY: 1999.

(20) Lian, C.; Janssen, M.; Liu, H.; van Roij, R., Blessing and Curse: How a Supercapacitor's Large Capacitance Causes its Slow Charging. *Phys. Rev. Lett.* **2020,** *124* (7), 076001.

(21) Kilic, M. S.; Bazant, M. Z.; Ajdari, A., Steric effects in the dynamics of electrolytes at large applied voltages. II. Modified Poisson-Nernst-Planck equations. *Phys. Rev. E Stat. Nonlin. Soft Matter Phys.* **2007,** *75* (2 Pt 1), 021503.

(22) Yang, J.; Janssen, M.; Lian, C.; van Roij, R., Simulating the charging of cylindrical electrolyte-filled pores with the modified Poisson-Nernst-Planck equations. *J. Chem. Phys.* **2022,** *156* (21), 214105.

(23) Ma, K.; Janssen, M.; Lian, C.; van Roij, R., Dynamic density functional theory for the charging of electric double layer capacitors. *J. Chem. Phys.* **2022,** *156* (8), 084101.

(24) Janssen, M., Transmission Line Circuit and Equation for an Electrolyte-Filled Pore of Finite Length. *Phys. Rev. Lett.* **2021,** *126* (13), 136002.

(25) Lian, C.; Su, H. P.; Li, C. Z.; Liu, H. L.; Wu, J. Z., Non-Negligible Roles of Pore Size Distribution on Electroosmotic Flow in Nanoporous Materials. *ACS nano* **2019,** *13* (7), 8185-8192.

(26) Futamura, R.; Iiyama, T.; Takasaki, Y.; Gogotsi, Y.; Biggs, M. J.; Salanne, M.; Segalini, J.; Simon, P.; Kaneko, K., Partial breaking of the Coulombic ordering of ionic liquids confined in carbon nanopores. *Nature Materials* **2017,** *16* (12), 1225-1232.

(27) Zuleta, M.; Björnbom, P.; Lundblad, A.; Nurk, G.; Kasuk, H.; Lust, E., Determination of diffusion coefficients of inside carbon nanopores using the single particle microelectrode technique. *J. Electroanal. Chem.* **2006,** *586* (2), 247-259.

(28) Zuleta, M.; Bursell, M.; Björnbom, P.; Lundblad, A., Determination of the effective diffusion coefficient of nanoporous carbon by means of a single particle microelectrode technique. *J. Electroanal. Chem.* **2003,** *549*, 101-108.

(29) Zuleta, M.; Bjornbom, P.; Lundblad, A.; Nurk, G.; Kasuk, H.; Lust, E., Determination of diffusion coefficients of BF4- inside carbon nanopores using the single particle microelectrode technique. *J. Electroanal. Chem.* **2006,** *586* (2), 247-259.

(30) Come, J.; Taberna, P. L.; Hamelet, S.; Masquelier, C.; Simon, P., Electrochemical Kinetic Study of LiFePO4 Using Cavity Microelectrode. *J. Electrochem. Soc.* **2011,** *158* (10), A1090-A1093.

(31) Kisu, K.; Iwama, E.; Naoi, W.; Simon, P.; Naoi, K., Electrochemical kinetics of nanostructure LiFePO4/graphitic carbon electrodes. *Electrochem. Commun.* **2016,** *72*, 10-14.

(32) Come, J.; Naguib, M.; Rozier, P.; Barsoum, M. W.; Gogotsi, Y.; Taberna, P. L.; Morcrette, M.; Simon, P., A Non-Aqueous Asymmetric Cell with a Ti2C-Based Two-Dimensional Negative Electrode. *J. Electrochem. Soc.* **2012,** *159* (8), A1368-A1373.

(33) Portet, C.; Chmiola, J.; Gogotsi, Y.; Park, S.; Lian, K., Electrochemical characterizations of carbon nanomaterials by the cavity microelectrode technique. *Electrochim. Acta* **2008,** *53* (26), 7675-7680.

(34) Clarisse Pe´an; Ce´line Merlet; Benjamin Rotenberg; Paul Anthony Madden; Pierre-Louis Taberna; Barbara Daffos; Mathieu Salanne; Simon, P., On the Dynamics of Charging in Nanoporous Carbon-Based Supercapacitors. *ACS nano* **2014,** *8*, 1576–1583.

(35) Cachet-Vivier, C.; Keddam, M.; Vivier, V.; Yu, L. T., Development of cavity microelectrode devices and their uses in various research fields. *J. Electroanal. Chem.* **2013,** *688*, 12-19.

(36) Cachet-Vivier, C.; Vivier, V.; Cha, C. S.; Nedelec, J. Y.; Yu, L. T., Electrochemistry of powder material studied by means of the cavity microelectrode (CME). *Electrochim. Acta* **2001,** *47* (1-2), 181-189.

(37) Lin, R.; Taberna, P. L.; Chmiola, J.; Guay, D.; Gogotsi, Y.; Simon, P., Microelectrode Study of Pore Size, Ion Size, and Solvent Effects on the Charge/Discharge Behavior of Microporous Carbons for Electrical Double-Layer Capacitors. *J. Electrochem. Soc.* **2009,** *156* (1), A7-A12.

(38) Lin, R.; Huang, P.; Segalini, J.; Largeot, C.; Taberna, P.-L.; Chmiola, J.; Gogotsi, Y.; Simon, P., Solvent effect on the ion adsorption from ionic liquid electrolyte into sub-nanometer carbon pores. *Electrochim. Acta* **2009,** *54* (27), 7025-7032.

(39) Tsai, W. Y.; Taberna, P. L.; Simon, P., Electrochemical Quartz Crystal Microbalance (EQCM) Study of Ion Dynamics in Nanoporous Carbons. *J. Am. Chem. Soc.* **2014,** *136* (24), 8722-8728.

(40) Wu, Y.-C.; Taberna, P.-L.; Simon, P., Tracking ionic fluxes in porous carbon electrodes from aqueous electrolyte mixture at various pH. *Electrochem. Commun.* **2018,** *93*, 119-122

(41) Dash, R.; Chmiola, J.; Yushin, G.; Gogotsi, Y.; Laudisio, G.; Singer, J.; Fischer, J.; Kucheyev, S., Titanium carbide derived nanoporous carbon for energy-related applications. *Carbon* **2006,** *44* (12), 2489-2497.

(42) Chmiola, J.; Yushin, G.; Gogotsi, Y.; Portet, C.; Simon, P.; Taberna, P. L., Anomalous increase in carbon capacitance at pore sizes less than 1 nanometer. *Science* **2006,** *313* (5794), 1760-1763.

(43) Yin, H.; Shao, H.; Daffos, B.; Taberna, P. L.; Simon, P., The effects of local graphitization on the charging mechanisms of microporous carbon supercapacitor electrodes. *Electrochem. Commun.* **2022,** *137*, 107258.

(44) Kondrat, S.; Kornyshev, A., Charging Dynamics and Optimization of Nanoporous Supercapacitors. *J. Phys. Chem. C* **2013,** *117* (24), 12399-12406.

(45) Mysyk, R.; Raymundo-Pinero, E.; Pernak, J.; Béguin, F. o., Confinement of symmetric tetraalkylammonium ions in nanoporous carbon electrodes of electric double-layer capacitors. *J. Phys. Chem. C* **2009,** *113* (30), 13443-13449.

(46) Ania, C. O.; Pernak, J.; Stefaniak, F.; Raymundo-Piñero, E.; Béguin, F., Polarization-induced distortion of ions in the pores of carbon electrodes for electrochemical capacitors. *Carbon* **2009,** *47* (14), 3158-3166.

(47) Eliad, L.; Salitra, G.; Soffer, A.; Aurbach, D., Ion sieving effects in the electrical double layer of porous carbon electrodes: estimating effective ion size in electrolytic solutions. *The Journal of Physical Chemistry B* **2001,** *105* (29), 6880-6887.

(48) Impey, R. W.; Madden, P. A.; Mcdonald, I. R., Hydration and Mobility of Ions in Solution. *J. Phys. Chem.* **1983,** *87* (25), 5071-5083.

(49) Rempe, S. B.; Pratt, L. R.; Hummer, G.; Kress, J. D.; Martin, R. L.; Redondo, A., The hydration number of Li^+ in liquid water. *J. Am. Chem. Soc.* **2000,** *122* (5), 966-967.

(50) Levi, M. D.; Levy, N.; Sigalov, S.; Salitra, G.; Aurbach, D.; Maier, J., Electrochemical Quartz Crystal Microbalance (EQCM) Studies of Ions and Solvents Insertion into Highly Porous Activated Carbons. *J. Am. Chem. Soc.* **2010,** *132* (38), 13220-13222.